
Current Concepts in Lymph Node Imaging*

Maha Torabi, MD; Suzanne L. Aquino, MD; and Mukesh G. Harisinghani, MD

Department of Radiology, Massachusetts General Hospital, Boston, Massachusetts

The accurate identification and characterization of lymph nodes by imaging has important therapeutic and prognostic significance in patients with newly diagnosed cancers. The presence of nodal metastases limits the therapeutic options and also generally indicates worse prognosis in patients. Thus, it becomes crucial to have this information before commencing therapy. Current cross-sectional imaging modalities rely on insensitive size and morphologic criteria and, thus, lack the desired accuracy for characterizing lymph nodes. This is mainly because metastases can be present in non-enlarged lymph nodes and not all enlarged nodes are malignant. PET has overcome some of these limitations but is still constrained by current resolution limits for small nodal metastases. This has fueled the development of targeted techniques for nodal imaging and characterization as outlined in this article. In the past few years, studies have shown that these newer imaging techniques can bridge some of the limitations of existing imaging for nodal characterization and thereby provide the much-needed staging information before the initiation of therapy.

Key Words: cancer staging; lymph node imaging; lymph node metastasis; malignant lymphadenopathy; nodal morphology; MRI; CT; PET; ultrasound

J Nucl Med 2004; 45:1509–1518

Once detected, most primary tumors are staged using the American Joint Committee on Cancer classification (1) to assess the local extent and size of the primary tumor (T), regional lymph node involvement (N), or distant metastasis (M). Evaluating the nodal status and staging of lymph nodes is important as nodal metastases in many types of primary cancer limit the therapeutic options and are also essential for determining the prognosis. In prostate cancer, for example, patients with nodal metastases are excluded from radical prostatectomy as a curative option and, instead, receive adjuvant therapy to achieve disease control (2). The number of lymph nodes infiltrated with malignant cells also has an impact in predicting a patient's survival outcome. For example, in breast cancer, involvement of 1–3 lymph nodes places a patient in N1 status with a 10-y survival rate of

>50%. However, involvement of ≥ 10 lymph nodes places a patient in stage IIIB or stage IV with a 10-y survival rate of <25% (3). Thus, it is important to accurately stage the lymph nodes in patients who are undergoing staging for primary cancer by means of either imaging modalities before surgery, as discussed in this article, or invasive surgical procedures. In certain malignancies in which imaging has a low accuracy, intraoperative exploration followed by frozen biopsy is used to sample lymph nodes at the time of primary tumor excision. Although this procedure of surgical staging with lymphadenectomy and careful histologic evaluation of the lymph nodes is considered as the gold standard in patients with various malignancies—for example, prostate cancer—this technique is invasive and limited by surgical field for nodal sampling. Moreover, this technique has limited accuracy—for example, as reported by Davis (4), in histologic analysis of intraoperative frozen section of lymph nodes, false-negative results as high as 33% have been reported in pelvic node analysis in prostate cancer patients. This necessitates the development of robust imaging techniques for nodal assessment before surgery.

Prior to the era of cross-sectional imaging, bipedal lymphography was the standard test for assessing and staging lymph nodes in the abdomen and pelvis. This technique evaluated and characterized lymph nodes based on changes in internal architecture (5). However, the procedure was invasive, laborious, and unable to consistently display lymph nodes above the level of the second lumbar vertebrae and outside the retroperitoneum. Lymphography has been effectively replaced by cross-sectional imaging, CT, and MRI. These modalities are routinely performed to assess the primary tumor and can readily display the lymph node along the drainage pathways of the tumor with much greater ease than lymphography.

The focus of this article is to briefly describe the evolution of imaging techniques from conventional anatomic modalities to molecular techniques in functional and physiologic assessment of lymph nodes.

ULTRASOUND (US)

Although widely available and easy to use, US has inherent limitations for imaging the lymph node groups in mediastinum, retroperitoneum, and deep pelvis. However, it has proven to be useful in assessment of cervical lymph nodes in patients with various head and neck carcinomas (6–8). Normal cervical nodes appear sonographically as

Received Mar. 31, 2004; revision accepted May 4, 2004.

For correspondence contact: Mukesh G. Harisinghani, MD, Department of Radiology, Division of Abdominal Imaging and Intervention, Massachusetts General Hospital, Boston, MA 02114.

E-mail: mharisinghani@partners.org

*NOTE: FOR CE CREDIT, YOU CAN ACCESS THIS ACTIVITY THROUGH THE SNM WEB SITE (http://www.snm.org/ce_online) THROUGH SEPTEMBER 2005.



FIGURE 1. US appearance of normal lymph node. Image shows flattened hypoechoic cigar-shaped structure (arrow).

somewhat flattened hypoechoic structures with varying amounts of hilar fat (9) (Fig. 1). They may show hilar vascularity but are usually hypovascular (10). Malignant infiltration alters the US features of the lymph nodes, resulting in enlarged nodes that are usually rounded and show peripheral or mixed vascularity (11) (Fig. 2). Using these features, US has been shown to have an accuracy of 89%–94% in differentiating malignant from benign cervical lymph nodes (12). In patients with thyroid cancer, for example, preoperative US evaluation of the cervical lymph nodes is not only accurate for detection of lymph node

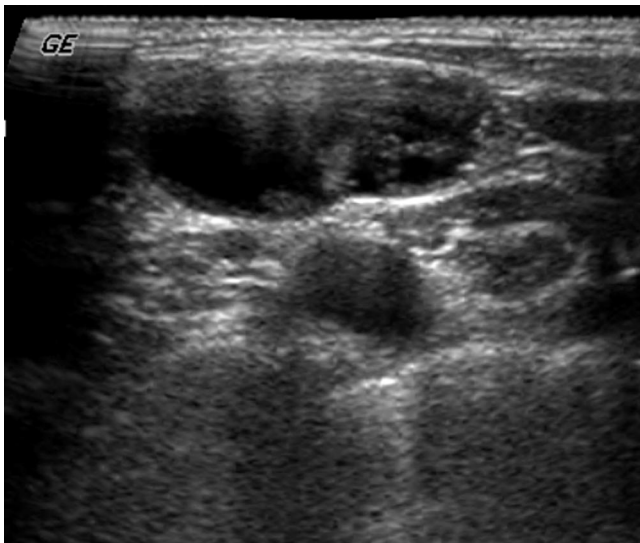


FIGURE 2. US appearance of malignant lymph node. Image shows enlarged round lymph node with mixed cystic and solid components in patient with metastatic papillary thyroid carcinoma.

metastases but also has been shown to alter the operative procedure in these patients, facilitating complete resection of disease and potentially minimizing locoregional recurrence (13). Wunderbaldinger et al. (14) evaluated cystic lymph node metastases in patients with papillary thyroid carcinoma and found, in most cases, that metastatic lymph nodes had thickened outer wall, internal echoes, internal nodularity, and septations.

Endoscopic US (EUS) has also been used to assess regional lymphadenopathy in esophageal, pancreatic, and rectal carcinomas. In a recent study, Saltzman (15) stated that EUS was the most accurate technique for the locoregional (T and N) staging of esophageal cancer, and optimal staging strategies for esophageal cancer should use EUS fine-needle aspiration with either CT or PET scans (15).

CROSS-SECTIONAL IMAGING

Current cross-sectional imaging modalities such as CT and MRI are noninvasive, have high patient acceptance, and require a short examination time. Because of these properties, these modalities have become the cornerstone for imaging various primary tumors. The assessment of lymph nodes using these modalities relies on lymph node anatomy rather than function and physiology. On cross-sectional imaging, a normal lymph node usually measures <1 cm in size, has a smooth and well-defined border, and shows uniform, homogeneous density or signal intensity. Most benign nodes have a central fatty hilum, which has a distinctive feature on CT and MRI (Figs. 3 and 4). Based on its anatomic location, the shape of a normal lymph node may vary. Usually normal nodes tend to have an oval or cigar shape. The primary yardstick for nodal staging by CT and MRI is lymph node size (Table 1), with the additional ability to assess for nodal morphology, signal intensity



FIGURE 3. Benign node with fatty hilum. Contrast-enhanced axial image of lower abdomen shows 9-mm aortocaval node (arrow) with central fatty hilum.

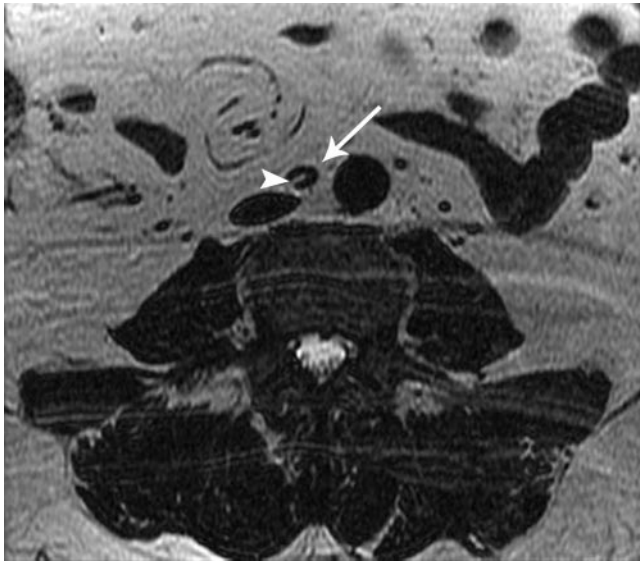


FIGURE 4. Axial T2-weighted image of lower abdomen shows 8-mm aortocaval node (arrow) with central fatty hilum (arrowhead).

changes, and dynamic gadolinium contrast enhancement on MRI. However, using size as the primary differentiating factor between benign and malignant nodes has limitations. It is difficult to establish a specific threshold value separating benign from malignant nodes, as a low size threshold provides higher sensitivity with low specificity and a higher size threshold lowers the sensitivity but improves specificity (22–24,26–28). A traditional size approach frequently overlooks metastasis, particularly when the metastasis involves only microscopic or partial infiltration of the lymph node. The specificity-of-size criterion also deteriorates because of benign inflammatory or infectious lymph node enlargement, leading to incorrect characterization of a benign lymph node as malignant. Based on the size criterion alone, MRI is no different (29) or slightly worse (30) than CT in the assessment of regional lymph node metastasis.

Clinical studies on cancer staging based on lymph node size using CT and MRI have had controversial results but, in general, the accuracy has been low (Table 2). Gagliardi et al. (25) found that in rectal cancer MRI has 67% sensitivity, 71% specificity, and 69% accuracy in detecting malignant lymphadenopathy. In evaluating uterine cancer, Bipat et al. (26) considered performance of CT and MR by reviewing 57 high-quality studies from 1985 to 2002 and concluded that sensitivity of MRI and CT for detecting lymph node involvement was 60% and 43%, respectively. Therefore, it has been concluded that lymph node size is not a reliable parameter for the evaluation of metastatic involvement (31–33).

The low accuracy reported with size parameters prompted the evaluation of nodal morphology on CT and MRI and signal intensity changes and dynamic enhancement parameters on MRI. The addition of morphologic criteria to the evaluation of lymph nodes seeks to exploit changes to the normal ovoid lymph node shape that arise from tumor infiltration. These changes could include either a more rounded shape, in which the long-to-short axis ratio decreases, or eccentric cortical hypertrophy (16,34). A commonly used size threshold in the pelvis accounts for this change in morphology, using 10 mm in short-axis diameter for ovoid lymph nodes while using a smaller threshold (8 mm) as a cutoff for rounded lymph nodes (34). In a study of 4,043 axillary lymph nodes in the setting of breast cancer, the use of either eccentric cortical hypertrophy or a long-axis diameter of >10 mm plus a long-to-short-axis ratio of <1.6 resulted in a sensitivity of 79% and a specificity of 93% for the detection of lymph node metastasis, with nearly all false-negative axillae demonstrating metastatic lymph nodes measuring <10 mm (16).

Several studies have investigated the utility of dynamic contrast-enhanced MRI for differentiating normal from metastatic lymph nodes (35,36). Simple comparison of signal intensity after intravenous gadolinium administration has not been effective in differentiating benign from malignant

TABLE 1
Summary of Literature Indicating Upper Size Limit for Benign Lymph Nodes According to Anatomic Site on Cross-Sectional Imaging

Anatomic site	Reference			Lymph node	
	Author	No.	Year	Maximum short-axis diameter (mm)	Maximum long-axis diameter (mm)
Axillary	Yoshimura et al.	(16)	1999	NA	10
Internal mammary	Kinoshita et al.	(17)	1999	NA	5
Pelvic	Vinnicombe et al.	(18)	1995	10	NA
Mediastinum	Ingram et al.	(19)	1989	10	NA
Jugulodigastric region	Van den Brekel et al.	(20)	1990	11	NA
Nonretropharyngeal nodes	Van den Brekel et al.	(20)	1990	10	NA
Lateral retropharyngeal	Van den Brekel et al.	(20)	1990	5	NA
Inguinal	Hawnaur et al.	(21)	2002	10	NA

NA = not applicable.

TABLE 2
Summary of Published Clinical Trials with CT/MRI

Reference			No. of patients	Region	CT/MRI		
Author	No.	Year			Sensitivity (%)	Specificity (%)	Accuracy (%)
Kau et al.	(22)	1999	70	Head and neck	65/88	47/41	NA
Dwamena et al.	(23)	1999	2,226	Lung	60/—*	77/—*	75/—*
Pieterman et al.	(24)	2000	102	Lung	75/—*	66/—*	69/—*
Gagliardi et al.	(25)	2002	28	Pelvic	—*/67	—*/71	—*/69
Bipat et al.	(26)	2003	NA	Uterine cervical	43/60	Both >90	NA
Anzai et al.	(27)	2003	147	All body regions	54	82	68
Antoch et al.	(28)	2003	27	Lung	70/—*	59/—*	63/—*

*This modality was not evaluated.
NA = not applicable.

lymph nodes (37). Rather, this approach relies on analysis of enhancement kinetics of the lymph node after bolus administration of gadolinium chelate agent and evaluates alterations in lymph node microcirculation such as flow characteristics, blood volume, microvascular permeability, and increased fractional volume of the extravascular extracellular space. Fischbein et al (36) evaluated cervical lymph nodes in 21 patients with squamous cell carcinoma of the head and neck. They found a significantly longer time to peak, lower peak enhancement, lower maximum slope, and slower washout slope in tumor-involved lymph nodes compared with normal lymph nodes. The authors concluded that in the malignant lymph node there is a decreased transfer of contrast material to the tissue and a reduced volume of extracellular space. They also indicated the difficulty in standardization of acquisition parameters to obtain reproducible data. In a study of mediastinal lymph nodes in 9 patients with bronchogenic carcinoma, Laissy et al. (38) found peak enhancement in metastatic lymph nodes within 60–80 s after gadolinium enhancement, with a slow washout thereafter. In contrast, reactive lymph nodes showed a gradual increase in contrast enhancement without a peak value in the first 6–8 min.

PET

With advanced innovations in functional imaging techniques, PET has great importance in lymph node imaging—primarily with the glucose analog ¹⁸F-FDG, which is avidly taken up by cells with increased rates of glycolysis. ¹⁸F-FDG is phosphorylated to ¹⁸F-FDG-6P, which is trapped in tumor cells that are relatively deficient in glucose-6-phosphatase during the time interval in which images are acquired. Numerous studies have demonstrated that ¹⁸F-FDG PET imaging has significantly improved the radiologic staging of some malignancies, especially lung cancer (Table 3). Pieterman et al. (24) demonstrated that the radiologic sensitivity and specificity of ¹⁸F-FDG PET was superior to CT in detecting malignant lymph nodes and staging of lung cancer. In their study, the sensitivity and specificity of PET was 91% and 86% compared with that of CT at 75% and 66% in detecting mediastinal metastases. However, the image resolution of PET is relatively low, which has been prohibitive in anatomic accuracy. The implementation of PET and CT fusion either by dual PET/CT or computer registration has evolved to overcome this obstacle (41,42). With fusion imaging, the accuracy of staging has improved. The superimposition of CT with high spatial resolution

TABLE 3
Summary of Published Clinical Trials with PET for Lymph Node Assessment

Reference			No. of patients	Region	PET		
Author	No.	Year			Sensitivity (%)	Specificity (%)	Accuracy (%)
Kau et al.	(22)	1999	70	Head and neck	87	94	*
Dwamena et al.	(23)	1999	514	Lung	79	91	92
Pieterman et al.	(24)	2000	102	Lung	91	86	87
Greco et al.	(39)	2001	167	Breast	94.4	86.3	89.8
Vesselle et al.	(40)	2002	118	Lung	80.9	96	90.7
Antoch et al.	(28)	2003	27	Lung	89	89	89

*Not measured.

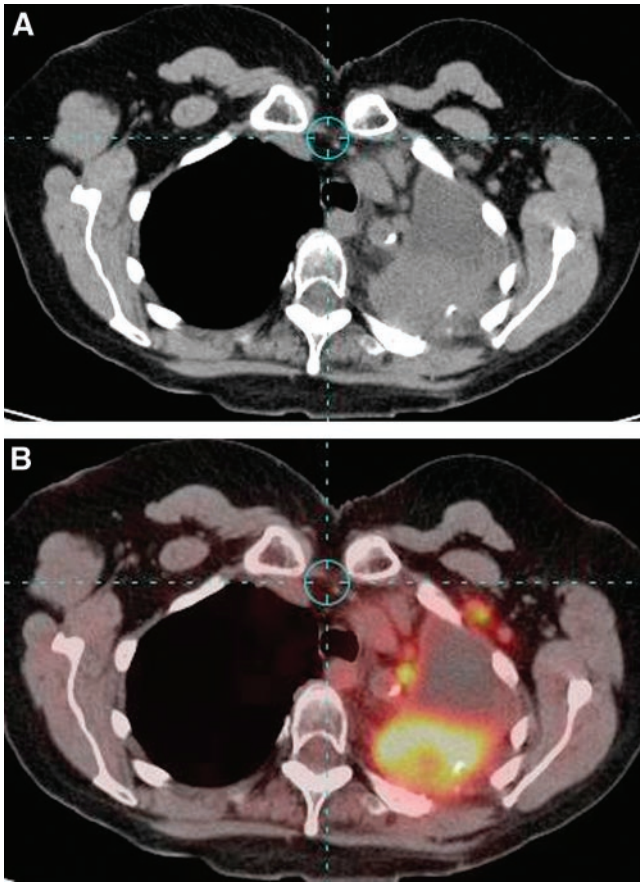


FIGURE 5. A 57-y-old woman with chest pain after lobectomy for lung cancer 4 mo earlier. (A) Axial CT scan shows mixed soft tissue and fluid in left pleural space. Prevascular and axillary lymph nodes were interpreted as normal. (B) Axial dual PET/CT scan shows increased uptake in soft-tissue mass as well as small prevascular and axillary lymph nodes, indicating recurrent disease with metastatic nodal spread.

improves the localization of areas of increased uptake within lymph nodes (Fig. 5). Lardinois et al. (41) reported an increase in accuracy of lung cancer staging with dual PET/CT compared with CT or PET interpreted alone. According to Aquino et al. (42), computer registration of CT

and PET datasets improved the specificity of mediastinal lymph node staging of lung cancer by better displaying lymph node metastases and aiding in detection of regions of ^{18}F -FDG accumulation due to physiologic (esophagus and blood pool) or inflammatory (atherosclerotic vessels) causes.

^{18}F -FDG PET has also been established in detecting the presence of recurrent malignancy. Posttherapy imaging is challenging because of anatomic distortion from surgery and radiation therapy. Areas of scar tissue may mimic or obscure early recurrence. ^{18}F -FDG PET has been useful in the surveillance of patients after treatment (43–45). Aquino et al. (46) found that image fusion of PET and CT improved the localization of recurrent thoracic disease in patients with lung cancer who received radiation therapy and surgery compared with PET interpretations without fusion. ^{18}F -FDG PET has improved the sensitivity and specificity of radiologic staging and restaging of lymphoma compared with gallium scintigraphy and CT (Fig. 6). According to Buchmann et al. (47), PET was significantly superior to CT in detecting tumor in patients with untreated lymphoma, especially above the diaphragm. In their study group, information from PET studies led to a change in therapy in 8%. Filmont et al. (48) reported that ^{18}F -FDG PET altered the clinical management of 35% of their patients with non-Hodgkin's lymphoma. They also reported that PET was significantly better at predicting disease-free survival than conventional imaging.

Urologic tumors have been particularly challenging in ^{18}F -FDG PET. For example, Hain and Maisey (49) found PET to have limited value in prostate cancer in differentiating between benign hypertrophic hyperplasia and adenocarcinoma. ^{11}C -Acetate and ^{11}C -methionine have shown potential as better agents for imaging prostate tumors. According to Oyama et al. (50), ^{11}C -acetate improves the detection of pelvic lymph nodes from prostate cancer compared with ^{18}F -FDG PET. ^{11}C -Acetate detected lymph node metastases in 5 patients compared with ^{18}F -FDG, which showed nodal disease 2 of the 5 patients. According to Macapinlac et al. (51), ^{11}C -methionine is superior to



FIGURE 6. Bilateral paraaortic nodes in patient with known lymphoma, seen on PET but only unilaterally on CT. (A) Axial contrast-enhanced CT scan shows enlarged right paraaortic node (arrow). (B) Coronal PET image shows bilateral areas of intense uptake suggestive of bilateral paraaortic malignant nodes (arrows).

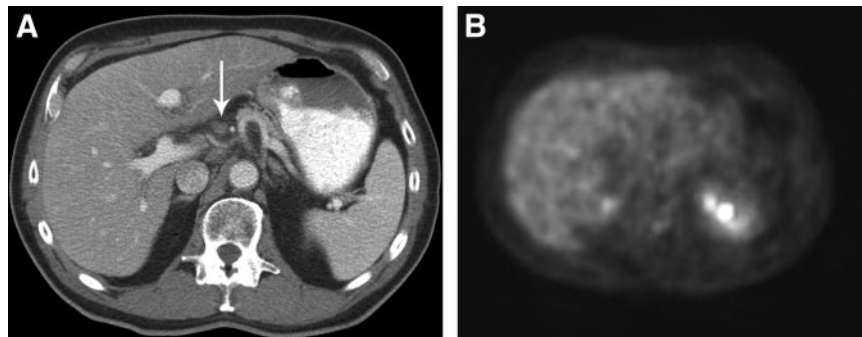


FIGURE 7. A 62-y-old man with pancreatic cancer. (A) CT scan shows prominent periportal lymph node (arrow). (B) Node did not show increased ^{18}F -FDG uptake. Cytology was positive for metastatic adenocarcinoma.

^{18}F -FDG imaging for prostate cancer due to the higher tumor-to-blood ratio and the earlier rapid uptake by tumor for earlier imaging. Also, the plateau of tumor uptake remains constant longer, allowing more uniform whole-body imaging.

Numerous clinical studies have shown that ^{18}F -FDG PET has limitations in accurately identifying malignant lymph nodes in the mediastinum. ^{18}F -FDG is not a very selective tracer for tumor imaging since cell types other than tumor cells actively use glucose. For example, macrophages that are found in inflammatory and infectious lesions can demonstrate increased ^{18}F -FDG uptake (52,53). Gupta et al. (54) found in their patient study group a lower sensitivity in detecting mediastinal lymph node metastases with PET due to the abnormal uptake of ^{18}F -FDG in lymph nodes involved with granulomatous disease or silicosis. The authors therefore recommend mediastinoscopy for pathologic correlation in any patients with abnormal lymph nodes on ^{18}F -FDG PET.

Numerous studies have shown that lymph nodes involved with bronchioloalveolar cell carcinoma and carcinoid tumors can give rise to false-negative results with ^{18}F -FDG PET (55–58). False-negative outcomes may also arise in lymph nodes that are <1 cm in diameter, are involved with well-differentiated tumors (Fig. 7), are located in close proximity to the primary tumor, or contain micrometastases (59,60). Rasanen et al. (61) found ^{18}F -FDG PET to be limited in the detection of locoregional lymph node metastases in esophageal carcinoma. Although the sensitivity in detecting the primary tumor was 84%, the sensitivity in detecting locoregional lymph nodes was 37% with 100% specificity. In certain malignancies, such as breast carcinoma and melanoma, surgical sentinel node biopsy has been

shown to be far superior to PET in detecting early micrometastases in draining lymph nodes. Barranger (62) reported a PET sensitivity of 20% in detecting sentinel lymph node disease. Van der Hoeven (63) reported an even poorer result, in which PET was falsely negative in all 18 patients with positive nodes on sentinel node biopsy. PET, however, was quite useful in detecting distant lymph node (Fig. 8), soft-tissue, and skeletal metastases for these same neoplasms and is, therefore, still a powerful imaging resource for staging.

^{18}F -FDG PET is just the beginning in the ongoing development of molecular imaging. Other radiopharmaceutical agents are being explored for potential oncology imaging, such as ^{11}C -acetate, ^{11}C -methionine, and ^{18}F -methyl choline for prostate cancer (64). Preliminary results show that ^{18}F -fluorothymidine, which images proliferating cells, is useful in detecting lung tumors (65,66). Studies are also under way for PET molecular imaging probes to monitor gene therapy (67,68).

NANOPARTICLE-ENHANCED MRI

The use of node-specific contrast agents can overcome some of the limitations of cross-sectional imaging. Ultra-small superparamagnetic iron oxide particles (USPIO) ([ferumoxtran-10] [Sinerem; Laboratoire Guerbet, Aulnay sous Bois; and Combidex; Advanced Magnetics]) are a relatively new class of MRI contrast agents developed in the 1980s for intravenous MR lymphography (69,70). These nanoparticles have been evaluated for improved detection of lymph node metastases in various clinical trials (27,71–75). Evaluation with nanoparticles requires 2 MR scans performed 24 h apart. The first scan is used to evaluate the

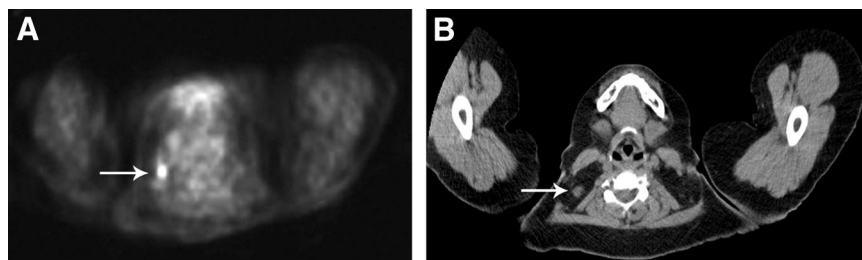


FIGURE 8. A 41-y-old woman with breast cancer. (A) PET/CT scan shows abnormal increased metabolism in right posterior cervical lymph node (arrow). (B) Cancer was missed on CT scan when it was interpreted without PET information (arrow).

existence and location of the lymph nodes. Twenty-four hours after the injection of the contrast agent, the second MR scan is performed to evaluate contrast enhancement of the identified lymph nodes.

After intravenous administration, ferumoxtran-10 extravasates slowly from the vascular space into the interstitial space and is then transported to lymph nodes through lymphatic vessels (Fig. 9). Once within the nodes, these nanoparticles bind to macrophages, producing a decrease in signal intensity on T2- and T2*-weighted images. The degree of signal intensity reduction is dependent on the dose of ferumoxtran-10 and the pulse sequence used for MRI. The recommended optimal dose at this time is 2.6 mg Fe per kilogram (76), and the most appropriate pulse sequence for evaluation of signal loss is the gradient-echo T2*-weighted sequence. This sequence is more sensitive to the magnetic susceptibility effects of ferumoxtran-10. If part of the node or the entire node is infiltrated with tumor, there is lack of ferumoxtran-10 uptake and these areas continue to retain their high signal intensity after administration of the contrast material. The spectrum of nodal enhancement patterns after ferumoxtran-10 administration depends on the nodal tumor burden ranging from homogeneous darkening to complete lack of ferumoxtran-10 uptake (Fig. 10). Reported false-negative results are usually due to microscopic foci of metastatic disease in small lymph nodes that are below the detection threshold of current MR scanners, and false-positive results are mainly due to reactive hyperplasia, localized nodal lipomatosis, and insufficient dosage of ferumoxtran-10. Despite these limitations, the reported accuracy of this novel technique supersedes the conventional parameters described earlier. Harisinghani et al. (71) reported a sensitivity of 100% with a specificity of 95.7% in characterizing lymph nodes in patients with prostate cancer. Anzai et al. (27), reporting on the overall phase III multicenter trial in evaluating various primary cancers, reported a sensitivity, specificity, and accuracy of 85%, 85%, and 85%, respectively, with postcontrast imaging alone and 83%, 77%, and 80%, respectively, with paired pre- and postcontrast MRI. The results of their study did not show a significant difference in diagnostic performance between postcontrast only and paired MRI, suggesting that it might be sufficient to obtain only postcontrast imaging for lymph node evaluation. Harisinghani et al. (77) also have shown that there is no statistically significant difference in evaluating lymph nodes when comparing postcontrast images alone with combined pre- and postcontrast images, and postcontrast images alone suffice for lymph node characterization (77). A summary of various reported series on ferumoxtran-10-enhanced MRI is shown in Table 4.

OTHER NOVEL TECHNIQUES

Research is currently underway to develop “smarter” agents that can aid in the visualization or detection of lymph node metastases. A novel macromolecular near-infrared flu-

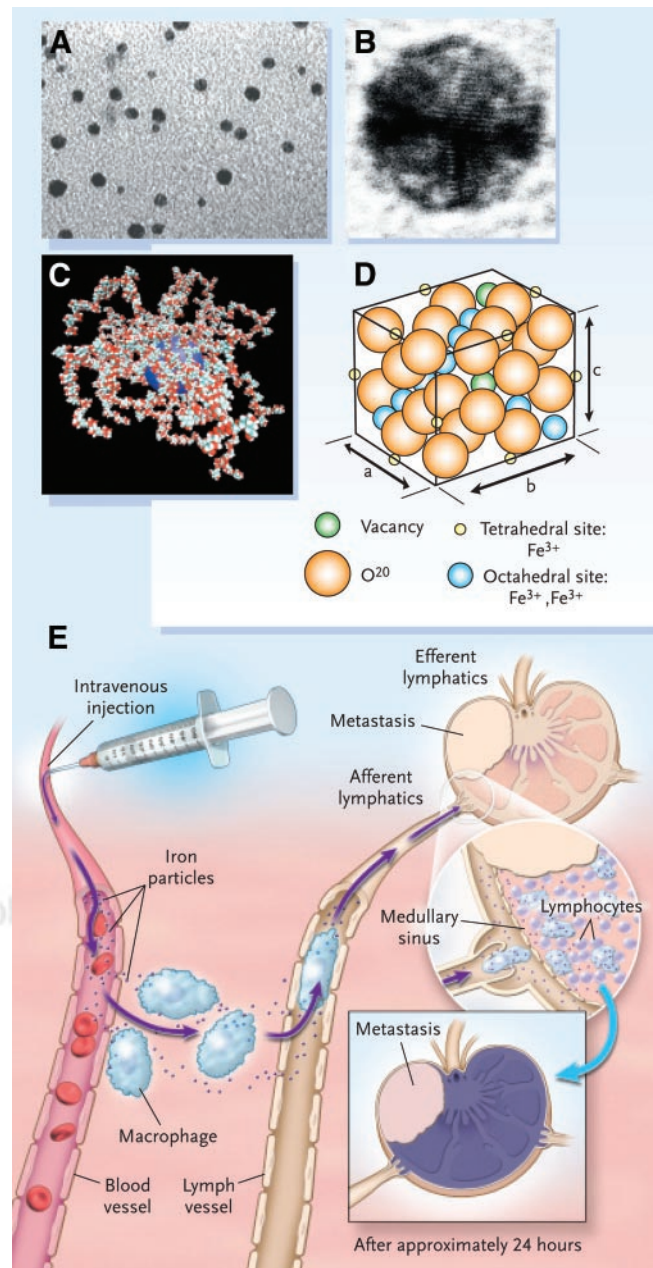


FIGURE 9. Electron microscopy and modeling of ferumoxtran-10. (A and B) Electron micrographs of superparamagnetic hexagonal nanoparticle crystal measuring 3 nm on average (A, bar = 10 nm; B, bar = 1 nm). (C and D) Molecular model of surface-bound 10-kDa dextrans (overall mean particle size, 28 nm) and iron oxide crystal packing. (E) Mechanism of action. Systemically injected long circulating particles gain access to interstitium and are drained ubiquitously through lymphatic vessels. Lymph flow disturbances or disturbances of nodal architecture by metastases lead to abnormal accumulation patterns, detectable by MRI. (Reprinted with permission of (71).)

orescent probe has been used in animal studies to visualize lymph nodes after intravenous administration (pan-node visualization) and subcutaneous administration (sentinel node visualization). This method was suggested to potentially serve as a method for guiding dissection with inter-

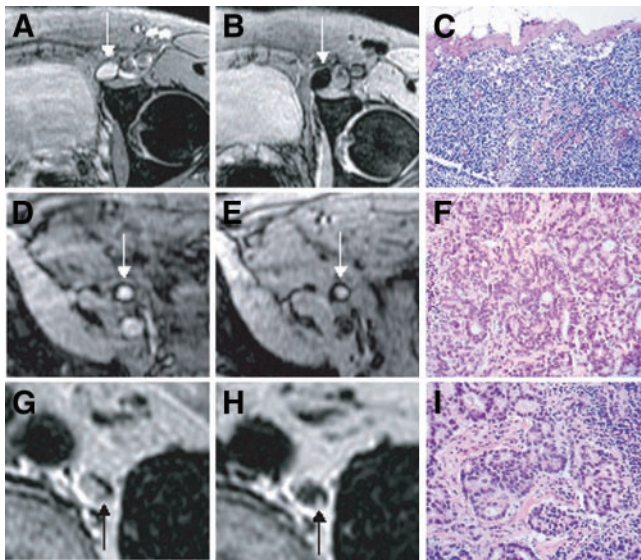


FIGURE 10. Spectrum of nodal signal intensity changes with magnetic nanoparticles. (A–C) Normal lymph node in left iliac region on noncontrast MR image (A) and 24 h after intravenous administration of ferumoxtran-10 (arrow) (B). Note homogeneous decrease in signal intensity due to ferumoxtran-10 accumulation. (C) Corresponding histology (10× objective). (D–F) Nonenlarged iliac lymph node completely replaced by tumor (arrow). (D) Conventional MR image shows high-signal-intensity lymph node. (E) Twenty-four hours after ferumoxtran-10 administration. Note that nodal signal intensity remains high. (F) Corresponding histology. (G–I) Micrometastases in retroperitoneal node. (G) MR image shows high-signal-intensity lymph node. (H) Ferumoxtran-10-enhanced MR image demonstrates 2 hyperintense foci (arrows) within node corresponding to 2-mm metastases. (I) Corresponding histology confirms presence of adenocarcinoma within node. (Reprinted with permission of (71).)

ventional radiologic and surgical procedures (80). Some peptides and antibodies have also been studied for immunohistochemical detection of lymph node metastases. Adrenomedullin (ADM) is an angiogenic factor that has also been shown to be a mitogen and a hypoxia survival factor for tumor cells. In one study, ADM peptide expression was examined in a series of malignant breast tumors by immu-

nohistochemistry using anti-ADM monoclonal antibody (81). It was shown that ADM peptide was widely expressed in breast cancer and that the degree of expression was associated with lymph node metastasis. Plasma ADM detected by radioimmunoassay could also represent an independent predictor of lymph node metastasis (81). Somatostatin receptor (SS-R) scintigraphy successfully has shown primary cancers and metastases in patients with a variety of SS-R-positive tumors. In vitro studies have shown that SS-Rs are present in lymph nodes from patients with Hodgkin's disease. Some studies support the validity of SS-R scanning as a powerful imaging technique for the staging of patients with Hodgkin's disease (82).

CONCLUSION

The important role of the radiologist in oncologic imaging is, first, to provide accurate pretreatment staging of the tumor for planning medical, surgical, and radiation interventions and, second, to monitor response to therapy and provide surveillance after curative treatment. Nodal staging forms an integral part of this process. Although controversy remains over the appropriate extent of preoperative imaging to assess lymph node status in a patient with malignancy, other factors should be considered based on the primary tumor, including accuracy and sensitivity of the modalities used for investigation, cost-effectiveness of each modality, and availability. Experience of the radiologist also plays a crucial role in acquisition and interpretation of the images.

With advances in technology, there is an inclination toward modalities that perform functional imaging of the lymph nodes rather than simply providing a cross-sectional view of the lymph node. PET/CT and MRI with nanoparticles provide both anatomic and functional information and are superior to modalities that provide solely anatomic or functional information. The added information from functional imaging of lymph node status will help optimize patient care by pinpointing the smallest tumor spread to the regional lymph nodes.

TABLE 4
Summary of Published Clinical Trials with USPIO

Reference			No. of patients	Region	USPIO		
Author	No.	Year			Sensitivity (%)	Specificity (%)	Accuracy (%)
Anzai et al.	(72)	1994	11	Ear, nose, and throat	95	84	*
Bellin et al.	(78)	1998	30	Pelvis retroperitoneum	100	80	*
Taupitz et al.	(73)	1999	50	Pelvis, abdomen	82	94	*
Taupitz et al.	(74)	1999	35	Breast	64	94	*
Sigal et al.	(79)	2002	81	Ear, nose, and throat	88	77	*
Anzai et al.	(27)	2003	147	All body regions	83	77	80
Harisinghani et al.	(71)	2003	80	Pelvis	90.5	95.7	*

*Not measured.

REFERENCES

- American Joint Committee on Cancer, American College of Surgeons. *AJCC Cancer Staging Manual*. 5th ed. Fleming ID, Cooper JS, Henson DE, et al., eds. Philadelphia, PA: American Cancer Society; 1997.
- Cheng L, Zincke H, Blute ML, Bergstralh EJ, Scherer B, Bostwick DG. Risk of prostate carcinoma death in patients with lymph node metastasis. *Cancer*. 2001; 91:66–73.
- Yarbro JW, Page DL, Fielding LP, Partridge EE, Murphy GP. American Joint Committee on Cancer Prognostic Factors Consensus Conference. *Cancer*. 1999; 86:2436–2446.
- Davis GL. Sensitivity of frozen section examination of pelvic lymph nodes for metastatic prostate carcinoma. *Cancer*. 1995;76:661–668.
- Guerhazi A, Brice P, Hennequin C, Sarfati E. Lymphography: an old technique retains its usefulness. *Radiographics*. 2003;23:1541–1558.
- Baatenburg de Jong RJ, Rongen RJ, De Jong PC, et al. Screening for lymph nodes in the neck with ultrasound. *Clin Otolaryngol*. 1988;13:5–9.
- Vassallo P, Wernecke K, Roos N, Peters PE. Differentiation of benign from malignant superficial lymphadenopathy: the role of high resolution US. *Radiology*. 1992;183:215–220.
- Vassallo P, Edel G, Roos N, et al. In-vitro high-resolution ultrasonography of benign and malignant lymph nodes: a sonographic-pathologic correlation. *Invest Radiol*. 1993;28:698–705.
- Marchal G, Oyen R, Verschakelen J, Gelin J, Baert AL, Stessens RC. Sonographic appearance of normal lymph nodes. *J Ultrasound Med*. 1985;4:417–419.
- Ying M, Ahuja A. Sonography of neck lymph nodes. Part I. Normal lymph nodes. *Clin Radiol*. 2003;58:351–358.
- Ahuja A, Ying M. Sonography of neck lymph nodes. Part II. Abnormal lymph nodes. *Clin Radiol*. 2003;58:359–366.
- Griffith JF, Chan AC, Ahuja AT, et al. Neck ultrasound in staging squamous oesophageal carcinoma: a high yield technique. *Clin Radiol*. 2000;55:696–701.
- Kouvaraki MA, Shapiro SE, Fornage BD, et al. Role of preoperative ultrasonography in the surgical management of patients with thyroid cancer. *Surgery*. 2003;134:946–954.
- Wunderbaldinger P, Harisinghani MG, Hahn PF, et al. Cystic lymph node metastases in papillary thyroid carcinoma. *AJR*. 2002;178:693–697.
- Saltzman JR. Section III: endoscopic and other staging techniques. *Semin Thorac Cardiovasc Surg*. 2003;15:180–186.
- Yoshimura G, Sakurai T, Oura S, et al. Evaluation of axillary lymph node status in breast cancer with MRI. *Breast Cancer*. 1999;6:249–258.
- Kinoshita T, Odagiri K, Andoh K, et al. Evaluation of small internal mammary lymph node metastases in breast cancer by MRI. *Radiat Med*. 1999;17:189–193.
- Vinnicombe SJ, Norman AR, Nicolson V, Husband JE. Normal pelvic lymph nodes: evaluation with CT after bipedal lymphangiography. *Radiology*. 1995; 194:349–355.
- Ingram CE, Belli AM, Lewars MD, Reznick RH, Husband JE. Normal lymph node size in the mediastinum: a retrospective study in two patient groups. *Clin Radiol*. 1989;40:35–39.
- Van den Brekel MW, Stel HV, Castelijns JA, et al. Cervical lymph node metastasis: assessment of radiologic criteria. *Radiology*. 1990;177:379–384.
- Hawnaur JM, Reynolds K, Wilson G, Hillier V, Kitchener HC. Identification of inguinal lymph node metastases from vulval carcinoma by magnetic resonance imaging: an initial report. *Clin Radiol*. 2002;57:995–1000.
- Kau RJ, Alexiou C, Laubenbacher C, Werner M, Schwaiger M, Arnold W. Lymph node detection of head and neck squamous cell carcinomas by positron emission tomography with fluorodeoxyglucose F 18 in a routine clinical setting. *Arch Otolaryngol Head Neck Surg*. 1999;125:1322–1328.
- Dwamena BA, Sonnad SS, Angobaldo JO, Wahl RL. Metastases from non-small cell lung cancer: mediastinal staging in the 1990s: meta-analytic comparison of PET and CT. *Radiology*. 1999;213:530–536.
- Pieterman RM, van Putten JW, Meuzelaar JJ, et al. Preoperative staging of non-small-cell lung cancer with positron-emission tomography. *N Engl J Med*. 2000;343:254–261.
- Gagliardi G, Bayar S, Smith R, Salem RR. Preoperative staging of rectal cancer using magnetic resonance imaging with external phase-arrayed coils. *Arch Surg*. 2002;137:447–451.
- Bipat S, Glas AS, van der Velden J, Zwinderman AH, Bossuyt PM, Stoker J. Computed tomography and magnetic resonance imaging in staging of uterine cervical carcinoma: a systematic review. *Gynecol Oncol*. 2003;91:59–66.
- Anzai Y, Piccoli CW, Outwater EK, et al. Evaluation of neck and body metastases to nodes with ferumoxtran 10-enhanced MR imaging: phase III safety and efficacy study. *Radiology*. 2003;228:777–788.
- Antoch G, Stattaus J, Nemat AT, et al. Non-small cell lung cancer: dual-modality PET/CT in preoperative staging. *Radiology*. 2003;229:526–533.
- Sohn KM, Lee JM, Lee SY, et al. Comparing MR imaging and CT in the staging of gastric carcinoma. *AJR*. 2000;174:1551–1557.
- Curtin HD, Ishwaran H, Mancuso AA, et al. Comparison of CT and MR imaging in staging of neck metastases. *Radiology*. 1998;207:123–130.
- Leslie A, Fyfe E, Guest P, Goddard P, Kabala JE. Staging of squamous cell carcinoma of the oral cavity and oropharynx: a comparison of MRI and CT in T- and N-staging. *J Comput Assist Tomogr*. 1999;23:43–49.
- Prenzel KL, Monig SP, Sinning JM, et al. Lymph node size and metastatic infiltration in non-small cell lung cancer. *Chest*. 2003;123:463–467.
- Tiguert R, Gheiler EL, Tefilli MV, et al. Lymph node size does not correlate with the presence of prostate cancer metastasis. *Urology*. 1999;53:367–371.
- Jager GJ, Barentsz JO, Oosterhof GO, et al. Pelvic adenopathy in prostatic and urinary bladder carcinoma: MR imaging with a three-dimensional T1-weighted magnetization-prepared-rapid gradient-echo sequence. *AJR*. 1996;167:1503–1507.
- Szabo BK, Aspelin P, Kristoffersen Wiberg M, Tot T, Bone B. Invasive breast cancer: correlation of dynamic MR features with prognostic factors. *Eur Radiol*. 2003;13:2425–2435.
- Fischbein NJ, Noworolski SM, Henry RG, Kaplan MJ, Dillon WP, Nelson SJ. Assessment of metastatic cervical adenopathy using dynamic contrast-enhanced MR imaging. *AJNR*. 2003;24:301–311.
- Kim SH, Kim SC, Choi BI, Han MC. Uterine cervical carcinoma: evaluation of pelvic lymph node metastasis with MR imaging. *Radiology*. 1994;190:807–811.
- Laissy JP, Gay-Depassier P, Soyer P, et al. Enlarged mediastinal lymph nodes in bronchogenic carcinoma: assessment with dynamic contrast-enhanced MR imaging—work in progress. *Radiology*. 1994;191:263–267.
- Greco M, Crippa F, Agresti R, et al. Axillary lymph node staging in breast cancer by 2-fluoro-2-deoxy-D-glucose-positron emission tomography: clinical evaluation and alternative management. *J Natl Cancer Inst*. 2001;93:630–635.
- Vesselle H, Pugsley JM, Vallieres E, Wood DE. The impact of fluorodeoxyglucose F 18 positron-emission tomography on the surgical staging of non-small cell lung cancer. *J Thorac Cardiovasc Surg*. 2002;124:511–519.
- Lardinois D, Weder W, Hany TF, et al. Staging of non-small-cell lung cancer with integrated positron-emission tomography and computed tomography. *N Engl J Med*. 2003;348:2500–2507.
- Aquino SL, Asmuth JC, Alpert NM, Halpern EF, Fischman AJ. Improved radiologic staging of lung cancer with 2-[¹⁸F]-fluoro-2-deoxy-D-glucose-positron emission tomography and computed tomography registration. *J Comput Assist Tomogr*. 2003;27:479–484.
- Karapetis CS, Strickland AH, Yip D, Steer C, Harper PG. Use of fluorodeoxyglucose positron emission tomography scans in patients with advanced germ cell tumour following chemotherapy: single-centre experience with long-term follow up. *Intern Med J*. 2003;33:427–435.
- Guay C, Lepine M, Verreault J, Benard F. Prognostic value of PET using ¹⁸F-FDG in Hodgkin's disease for posttreatment evaluation. *J Nucl Med*. 2003; 44:1225–1231.
- Anderson GS, Brinkmann F, Soulen MC, Alavi A, Zhuang H. FDG positron emission tomography in the surveillance of hepatic tumors treated with radiofrequency ablation. *Clin Nucl Med*. 2003;28:192–197.
- Aquino SL, Asmuth JC, Moore RH, Weise SB, Fischman AJ. Improved image interpretation with registered thoracic CT and positron emission tomography data sets. *AJR*. 2002;178:939–944.
- Buchmann I, Reinhardt M, Elsner K, et al. 2-(Fluorine-18)fluoro-2-deoxy-D-glucose positron emission tomography in the detection and staging of malignant lymphoma: a bicenter trial. *Cancer*. 2001;91:889–899.
- Filmont JE, Vranjesevic D, Quon A, et al. Conventional imaging and 2-deoxy-2-[¹⁸F]fluoro-D-glucose positron emission tomography for predicting the clinical outcome of previously treated non-Hodgkin's lymphoma patients. *Mol Imaging Biol*. 2003;5:232–239.
- Hain SF, Maisey MN. Positron emission tomography for urological tumours. *BJU Int*. 2003;92:159–164.
- Oyama N, Akino H, Kanamaru H, et al. ¹¹C-Acetate PET imaging of prostate cancer. *J Nucl Med*. 2002;43:181–186.
- Macapinlac HA, Humm JL, Akhurst T, et al. Differential metabolism and pharmacokinetics of L-[1-¹¹C]-methionine and 2-[¹⁸F]fluoro-2-deoxy-D-glucose (FDG) in androgen independent prostate cancer. *Clin Positron Imaging*. 1999;2: 173–181.
- Kapucu LO, Meltzer CC, Townsend DW, Keenan RJ, Luketich JD. Fluorine-18-fluorodeoxyglucose uptake in pneumonia. *J Nucl Med*. 1998;39:1267–1269.
- Rennen HJ, Corstens FH, Oyen WJ, Boerman OC. New concepts in infection/inflammation imaging. *Q J Nucl Med*. 2001;45:167–173.
- Gupta NC, Tamim WJ, Graeber GG, Bishop HA, Hobbs GR. Mediastinal lymph node sampling following positron emission tomography with fluorodeoxyglucose imaging in lung cancer staging. *Chest*. 2001;120:521–527.

55. Higashi K, Ueda Y, Seki H, et al. Fluorine-18-FDG PET imaging is negative in bronchioloalveolar lung carcinoma. *J Nucl Med.* 1998;39:1016–1020.
56. Heyneman LE, Patz EF. PET imaging in patients with bronchioloalveolar cell carcinoma. *Lung Cancer.* 2002;38:261–266.
57. Jadvar H, Segall GM. False-negative fluorine-18-FDG PET in metastatic carcinoma. *J Nucl Med.* 1997;38:1382–1383.
58. Erasmus JJ, McAdams HP, Patz EF Jr, Coleman RE, Ahuja V, Goodman PC. Evaluation of primary pulmonary carcinoid tumors using FDG PET. *AJR.* 1998;170:1369–1373.
59. Kostakoglu L, Agress H Jr, Goldsmith SJ. Clinical role of FDG PET in evaluation of cancer patients. *Radiographics.* 2003;23:315–340.
60. Ruers TJ, Langenhoff BS, Neeleman N, et al. Value of positron emission tomography with [F-18]fluorodeoxyglucose in patients with colorectal liver metastases: a prospective study. *J Clin Oncol.* 2002;20:388–395.
61. Rasanen JV, Sihvo EIT, Knuuti MJ, et al. Prospective analysis of accuracy of positron emission tomography, computed tomography, and endoscopic ultrasonography in staging of adenocarcinoma of the esophagus and the esophago-gastric junction. *Ann Surg Oncol.* 2003;10:954–960.
62. Barranger E, Grahek D, Antoine M, Montravers F, Talbot J-N, Uzan S. Evaluation of fluorodeoxyglucose positron emission tomography in the detection of axillary lymph node metastases in patients with early-stage breast cancer. *Ann Surg Oncol.* 2003;10:622–627.
63. Van der Hoeven JJ, Hoekstra OS, Comans EF, et al. Determinants of diagnostic performance of [F-18]fluorodeoxyglucose positron emission tomography for axillary staging in breast cancer. *Ann Surg.* 2002;236:619–624.
64. DeGrado TR, Coleman RE, Wang S, et al. Synthesis and evaluation of ¹⁸F-labeled choline as an oncologic tracer for positron emission tomography: initial findings in prostate cancer. *Cancer Res.* 2001;61:110–117.
65. Buck AK, Halter G, Schirmer H, et al. Imaging proliferation in lung tumors with PET: ¹⁸F-FLT versus ¹⁸F-FDG. *J Nucl Med.* 2003;44:1426–1431.
66. Dittmann H, Dohmen BM, Paulsen F, et al. [¹⁸F]FLT PET for diagnosis and staging of thoracic tumours. *Eur J Nucl Med Mol Imaging.* 2003;30:1407–1412.
67. Ray P, Wu AM, Gambhir SS. Optical bioluminescence and positron emission tomography imaging of a novel fusion reporter gene in tumor xenografts of living mice. *Cancer Res.* 2003;63:1160–1165.
68. Gambhir SS, Bauer E, Black ME, et al. A mutant herpes simplex virus type 1 thymidine kinase reporter gene shows improved sensitivity for imaging reporter gene expression with positron emission tomography. *Proc Natl Acad Sci USA.* 2000;97:2785–2790.
69. Weissleder R, Elizondo G, Wittenberg J, Rabito CA, Bengel HH, Josephson L. Ultrasmall superparamagnetic iron oxide: characterization of a new class of contrast agents for MR imaging. *Radiology.* 1990;175:489–493.
70. Lee AS, Weissleder R, Brady TJ, Wittenberg J. Lymph nodes: microstructural anatomy at MR imaging. *Radiology.* 1991;178:519–522.
71. Harisinghani MG, Barentsz J, Hahn PF, et al. Noninvasive detection of clinically occult lymph-node metastases in prostate cancer. *N Engl J Med.* 2003;348:2491–2499.
72. Anzai Y, Blackwell KE, Hirschowitz SL, et al. Initial clinical experience with dextran-coated superparamagnetic iron oxide for detection of lymph node metastases in patients with head and neck cancer. *Radiology.* 1994;192:709–715.
73. Taupitz M, Hamm BK, Barentsz JO, Vock P, Roy C, Bellin MF. Sinerem®-enhanced MRI imaging compared to plain MR imaging in evaluating lymph node metastases from urologic and gynecologic cancers [abstract]. *Proceedings of the Radiological Society of North America*; Chicago, IL; November 29–December 3, 1999. 213(P):387.
74. Taupitz M, Wallis F, Heywang-Koebrunner SH, Thibault F, Gilles R, Tardivon AA. Axillary lymph node MR imaging with Sinerem® in patients with suspected breast cancer [abstract]. *Proceedings of the Radiological Society of North America*; Chicago, IL; November 29–December 3, 1999. 213(P):369.
75. Harisinghani MG, Saini S, Weissleder R, et al. MR lymphangiography using ultrasmall superparamagnetic iron oxide in patients with primary abdominal and pelvic malignancies: radiographic-pathologic correlation. *AJR.* 1999;172:1347–1351.
76. Hudgins PA, Anzai Y, Morris MR, Lucas MA. Ferumoxtran-10, a superparamagnetic iron oxide as a magnetic resonance enhancement agent for imaging lymph nodes: a phase 2 dose study. *AJNR.* 2002;23:649–656.
77. Harisinghani M, Deserno W, Hahn PF, Barentsz J, Perumpilichirra J, Weissleder R. MR lymphangiography for detection of minimal nodal disease in patients with prostate cancer: does postcontrast imaging alone suffice for accurate characterization [abstract]? *Proceedings of the Radiological Society of North America*; Chicago, IL; December 1–6, 2002. *Radiology*; 225(P):350.
78. Bellin MF, Roy C, Kinkel K, et al. Lymph node metastases: safety and effectiveness of MR imaging with ultrasmall superparamagnetic iron oxide particles—initial clinical experience. *Radiology.* 1998;207:799–808.
79. Sigal R, Vogl T, Casselman J, et al. Lymph node metastases from head and neck squamous cell carcinoma: MR imaging with ultrasmall superparamagnetic iron oxide particles (Sinerem MR)—results of a phase-III multicenter clinical trial. *Eur Radiol.* 2002;12:1104–1113.
80. Josephson L, Mahmood U, Wunderbaldinger P, et al. Pan and sentinel lymph node visualization using a near-infrared fluorescent probe. *Mol Imaging.* 2003; 2:18–23.
81. Oehler MK, Fischer DC, Orlowska-Volk M, et al. Tissue and plasma expression of the angiogenic peptide adrenomedullin in breast cancer. *Br J Cancer.* 2003; 89:1927–1933.
82. Lugtenburg PJ, Krenning EP, Valkema R, et al. Somatostatin receptor scintigraphy useful in stage I-II Hodgkin's disease: more extended disease identified. *Br J Haematol.* 2001;112:936–944.